

Chapter 8

Desiccant Air Handling Processors Driven by Heat Pump

Tao Zhang, Rang Tu and Xiaohua Liu

Abstract Desiccant air handling processors (DAHP) driven by heat pump have become more and more popular recently due to their compact size and high efficiency. Both the cooling capacity from an evaporator and heat from a condenser are utilized in these systems. How to understand these two kinds of air dehumidification systems comprehensively is an important issue for system design and device selection. In the present chapter, DAHP driven by heat pump (using liquid desiccant or desiccant wheel) will be investigated. Operating principles of DAHP using desiccants will be introduced firstly. System design principles will be proposed with emphasis on the heat and mass transfer characteristics in DAHP. Performances of DAHP will be analyzed and approaches for performance optimization will also be proposed. It is expected that the present study will be useful to cast light on the performances of DAHP using liquid desiccant and desiccant wheel and choose an efficient air dehumidification method in the air-conditioning system.

Keywords Air handling process · Liquid desiccant · Desiccant wheel · Heat pump · Energy performance

8.1 Introduction

Nowadays energy consumed in buildings is an important composition of the total energy consumption in society, as well as the energy consumed by industry or transportation. In China about 20% of the entire energy is consumed by buildings, which is still in rapid progress with the development of economy and society [1]. In commercial buildings, about 30–60% of the total energy is consumed by the

T. Zhang (✉) · X. Liu
Department of Building Science, Tsinghua University, Beijing 100084, China
e-mail: zt2015@tsinghua.edu.cn

R. Tu
School of Mechanical Engineering, University of Science and Technology Beijing,
Beijing 100083, China

air-conditioning system [1]. Air dehumidification device is an important component of the air-conditioning system, which is more important in humid regions. It is of great importance to improve the energy performance of air dehumidification devices in reducing building energy consumption. In contrast to the conventional condensing dehumidification method, air dehumidification processes using liquid desiccant (LD) and solid desiccant including desiccant wheel (DW) are becoming more and more popular. It is believed that the air dehumidification systems using desiccant are with superiority in not requiring reheat, utilization of waste heat and etc.

Characteristics of liquid desiccant and desiccant material are treated as the fundamental researches for supporting the development of air handling systems using desiccant [2–4]. Both theoretical models [5] and experimental results [6, 7] have been investigated intensively for the coupled heat and mass transfer processes between air and liquid desiccant or solid desiccant. The basic principle for the air handling processes using LD and DW is to realize humidification or dehumidification with the help of the water vapor pressure difference between air and desiccant. The common aqueous solutions mainly include lithium chloride (LiCl), lithium bromide (LiBr) and calcium chloride (CaCl₂) aqueous solutions, while the common solid desiccants include silica gel, zeolite and so on. The solution state could be expressed by the humid air in equilibrium with the desiccant (with the same temperature and vapor pressure). Figure 8.1a illustrates the LiBr aqueous solution in the air psychrometric chart, where X represents the solution concentration and ϕ denotes the relative humidity. It is indicated that the iso-concentration line of the liquid desiccant coincides with the air iso-relative humidity line. It can reach a larger area compared to water (which is located at the 100% saturated state of air). Similarly state of the solid desiccant could also be presented in an air psychrometric chart, shown in Fig. 8.1b, where W indicates the water content.

The coupled heat and mass transfer processes between air and liquid desiccant in a packed tower is illustrated in Fig. 8.2a, with the air handling process shown in the psychrometric chart in Fig. 8.2b. Variance of the solution concentration is usually

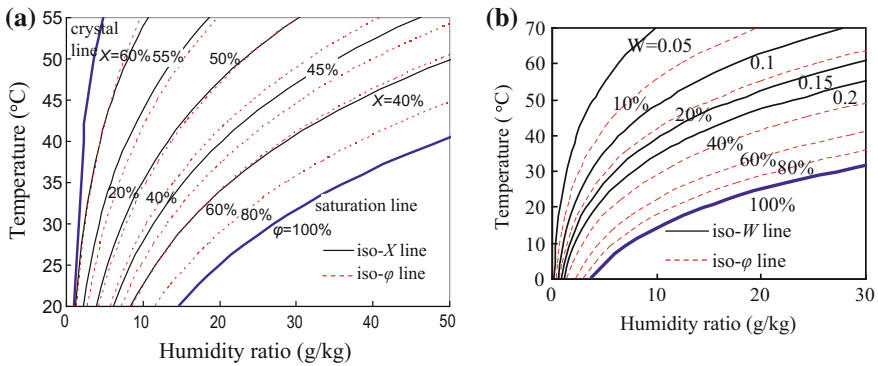


Fig. 8.1 Desiccant states shown in the air psychrometric chart: **a** LiBr solution; and **b** RD silica gel [8]

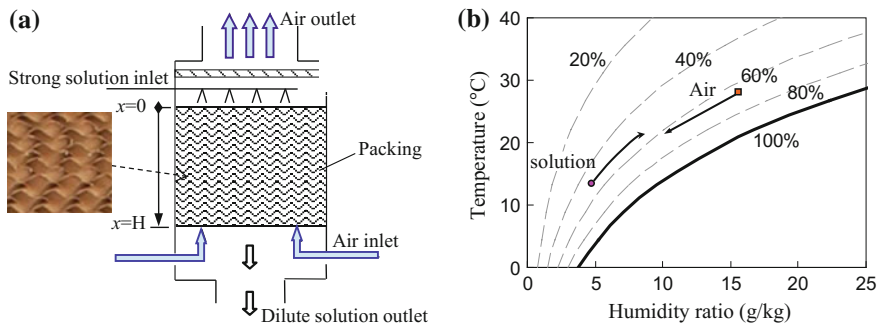


Fig. 8.2 Counter flow process between air and liquid desiccant: **a** operating principle; and **b** air handling process shown in the air psychrometric chart

lower than 1% for the coupled heat and mass transfer processes between air and solution [9]. The solution state could be regarded as almost varying along the iso-concentration line. There could be various inlet air states relative to the solution state, with handling results such as dehumidification or humidification.

Desiccant wheel system is the common method using solid desiccant for air dehumidification and Fig. 8.3a presents its operating principle. Driving force for the mass transfer process is precisely the vapor pressure (or humidity ratio) difference between air and solid desiccant. Porous material is utilized as the substrate with superiority in increasing the specific surface area. There is an obvious gap between the reachable number of transfer unit NTU (equaling to the transfer ability hA divided by the heat capacity $c_p m$) of LD system and DW system. The air side NTU of the DW process is significantly higher than that of the LD process at the same volume. The specific area of DW could be as high as $2000\text{--}4000\text{ m}^2/\text{m}^3$. For example, the NTU for the air side is about 5–10 as the thickness of DW is about 10 cm with an air velocity of about 2 m/s. While the specific surface area the

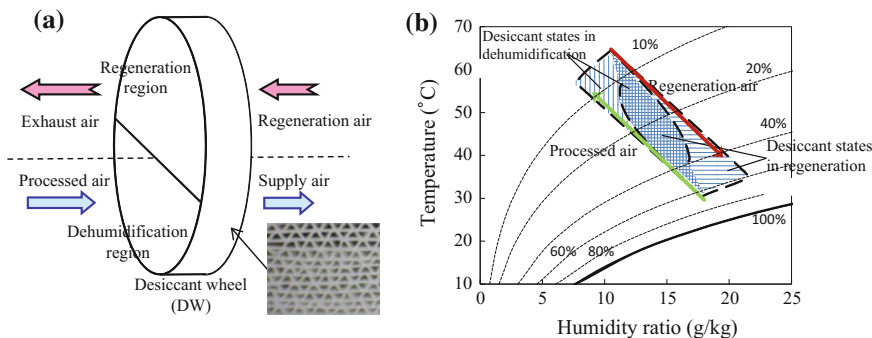


Fig. 8.3 Air handling process using desiccant wheel: **a** operating principle; and **b** air handling process shown in the air psychrometric chart

packing in the LD process is usually lower than $1000 \text{ m}^2/\text{m}^3$, the NTU for the air side is only about 1–3. There are dehumidification region and regeneration region along the circumference of the wheel. Moisture is transferred from the air to the desiccant in the dehumidification region with the release of adsorption heat, and from the desiccant to the regeneration air in the regeneration region. The air handling process in the DW process is illustrated in Fig. 8.3b, where the air state varies almost along the isenthalpic line. The air is usually heated to satisfy the heating requirement for desiccant regeneration.

On basis of the performance investigation between air and liquid desiccant or solid desiccant, novel systems and handling devices using LD or DW are also proposed and investigated. Desiccant air handling processors (DAHP) driven by heat pump have become more and more popular recently due to their compact size and high efficiency. Both the cooling capacity from an evaporator and heat from a condenser are utilized in these systems. Taking liquid desiccant as an example, the cooling capacity is used to cool the circulating desiccant to enhance its dehumidification ability and the heat is used to regenerate the desiccant.

Current researches provide sufficient basis to analyze the characteristics of air handling process using either LD or DW. How to understand these two kinds of air dehumidification systems comprehensively is an important issue for system design and device selection. There is seldom study focusing on the comparable performances of these systems, to the disadvantage of a fully understanding on DAHP driven by heat pump. The mathematical models for LD systems and DW systems have been built and validated in the previous studies [10, 11]. In the present chapter, DAHP driven by heat pump (using LD or DW) will be investigated. System design principles will be proposed with emphasis on the heat and mass transfer characteristics in DAHP. It is expected that the present study will be useful to cast light on the performances of DAHP using LD and DW and choose an efficient air dehumidification method in the air-conditioning system.

8.2 Air Handling Process Using Liquid Desiccant

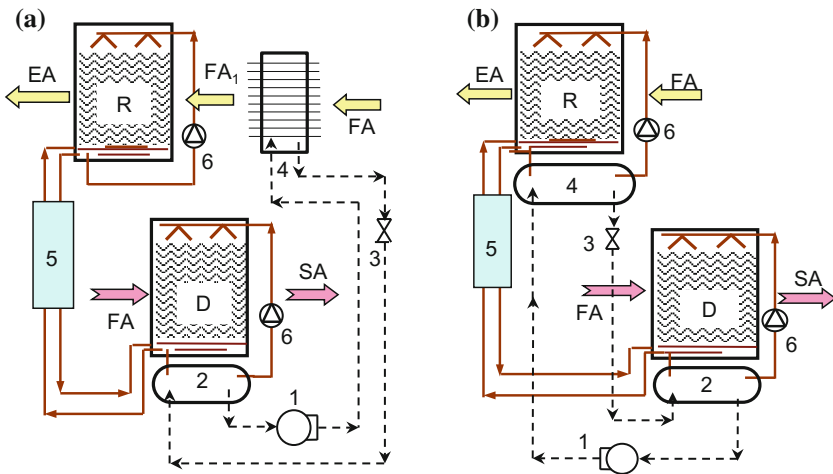
8.2.1 Basic Handling Process and Theoretical Analysis

For air handling processor driven by heat pump using liquid desiccant, there are different ways to utilize the condensing heat for desiccant regeneration. All the condensing heat from the heat pump could put in the solution for regeneration. While all the condensing heat from the heat pump could be removed by the regeneration air rather than by the solution, and the heated air went into the regenerator for desiccant regeneration. The issues of how to evaluate the performances of different HPLD systems and how to pursue a process with better energy efficiency are at the center of current research efforts. There are various kinds of HPLD systems in which condensing heat is usually utilized for desiccant

regeneration, and the cooling capacity of the evaporator is adopted for dehumidification. However, to obtain better mass transfer performance, previous studies have recommended that the cooling capacity should be used to cool the inlet solution rather than the air in the dehumidification process [9]. Accordingly, in the processes analyzed in the present study, the evaporator of the heat pump is utilized to cool the solution for dehumidification.

Figure 8.4a, b shows the operating schematics of two basic HPLD processes. In these processes, an adiabatic dehumidifier/regenerator is adopted. A small part of the diluted solution after dehumidification is sent into the regenerator, and there is also a small amount of concentrated solution after regeneration returning back to the dehumidifier. As the variance of the desiccant concentration is usually lower than 1% [9], the mass flow rates of these two parts of solutions circulating between the dehumidifier and the regenerator are almost the same for these HPLD systems. The solution heat recovery device is used for the heat recovery between the diluted solution sent to the regenerator and the concentrated solution sent to the dehumidifier. The concentrated solution sent to the dehumidifier is then mixed with the rest of the diluted solution after dehumidification and sent to the top of the dehumidifier with the help of a solution pump.

In contrast to the typical adiabatic process where all the solution circulates between the dehumidifier and the regenerator, in the adiabatic dehumidifier/regenerator investigated in the present study, most of the solution circulates only between the packed tower and the evaporator or condenser. The major difference between Basic



FA-fresh air; *SA*-supply air; *FA₁*-fresh air heated by the condenser; *EA*-exhaust air; *D*-dehumidifier; *R*-regenerator; 1-compressor; 2-evaporator; 3-expansion valve; 4-condenser; 5-heat exchanger; 6-pump.

Fig. 8.4 Operating schematic of the HPLD air handling processes with different regeneration modes: **a** Basic Type I (heat inlet air); and **b** Basic Type II (heat inlet solution)

Type I and Basic Type II systems is that the condenser is used for heating different fluids. In Basic Type I, the condenser is an air-cooled type, and the regeneration air is heated by the condensing heat before flowing through the regenerator. A solution-cooled condenser is adopted in Basic Type II, and the solution is heated by the condensing heat instead of the regeneration air.

COP_{hp} and COP_{sys} are chosen as indexes to evaluate the performances of various HPLD systems, calculated by Eqs. (8.1) and (8.2), respectively:

$$COP_{hp} = \frac{Q_{evap}}{P_{com}} \quad (8.1)$$

$$COP_{sys} = \frac{Q_a}{P_{com} + P_{pump}} \quad (8.2)$$

where Q_{evap} and Q_a represent the cooling capacities of evaporator and processed air, respectively; P_{com} and P_{pump} indicate the power consumptions of compressor and solution pumps involved in the handling process, respectively.

There are several key components in the HPLD systems, including the coupled heat and mass transfer components (the dehumidifier and regenerator), the heat pump system, the heat exchanger, etc. On basis of the theoretical models of these key components, a system model for the HPLD process can be established. In previous research [12], a model of this kind of HPLD system was built and the flow chart of the calculating method was also given; to validate the system models, the tested results and simulated results of a three-stage HPLD system were investigated, including the supply air temperature, humidity ratio, compressor power and COP_{hp} . It showed that the mean relative biases between the measured and simulated results of the HPLD device were all lower than 10% and the simulated results showed good agreement with the measured. Thus, the theoretical models of the various components were validated and the system models could be used to analyze the performance of different HPLD systems.

The system simulation method helps to calculate the performance parameters of HPLD systems. However, a simple solution for evaluating performance discrepancies is still lacking. To simplify the comparison of different HPLD systems, the current study investigates the match properties in the key components of the HPLD systems. The unmatched coefficient based on entransy dissipation is adopted, including the sensible heat transfer process and the coupled heat and mass transfer processes. Dissipations occur during the heat and mass transfer processes of the air-desiccant packed tower due to limited transfer capability, flow mismatching, and parameter mismatching, similar to the air-water process [13].

To depict the characteristics of driving forces between air and desiccant, exergy analysis method and unmatched coefficient are adopted as the theoretical indexes. It is indicated that the exergy is provided by the cooling source (ΔE_{wc}), heating source (ΔE_{wh}), and the regeneration air (ΔE_{ca}), and exergy consumption consists of two parts. Part of the exergy is used to increase the exergy of the processed air (ΔE_{sa}). The rest is destroyed during the heat or mass transfer processes in dehumidifier/regenerator

($\Delta E_{de,deh}/\Delta E_{de,reg}$) and heat exchangers ($\Delta E_{de,he}$). Thus, the exergy balance equation of the LD system I can be written as Eq. (8.3):

$$\Delta E_{wc} + \Delta E_{wh} + \Delta E_{ea} = \Delta E_{sa} + \Delta E_{de,deh} + \Delta E_{de,reg} + \Delta E_{de,HE} \quad (8.3)$$

where the subscript *wc* refers to cooling source (evaporator), *wh* denotes heating source (condenser), *ea* refers to regeneration air, *sa* denotes supply air, *de* refers to exergy destruction, *deh* denotes dehumidifier, *reg* represents regenerator, and *HE* refers to heat exchangers including solution–solution heat exchanger and air–water heat exchanger.

The exergy of humid air at standard atmospheric pressure is the sum of thermal exergy and humid exergy, expressed as Eq. (8.4) [14].

$$\begin{aligned} ex_a = & (c_{p,a} + \omega c_{p,v})T_0 \left(\frac{T}{T_0} - 1 - \ln \frac{T}{T_0} \right) \\ & + R_a T_0 \left((1 + 1.608\omega) \ln \frac{1 + 1.608\omega}{1 + 1.608\omega_0} + 1.608\omega \ln \frac{\omega}{\omega_0} \right) \end{aligned} \quad (8.4)$$

where R_a is gas constant for air; subscript *R* represents reference point of exergy. The reference temperature T_0 is chosen as the outdoor air temperature, and the reference humidity ratio ω_0 is chosen as the saturated humidity ratio of the reference temperature [15].

As for the air handling process between air and solution, its exergy destruction ΔE_{de} is composed of the exergy destruction of sensible heat transfer ($\Delta E_{de,h}$) and that of moisture transfer ($\Delta E_{de,m}$), calculated by Eqs. (8.5)–(8.7) [16].

$$\Delta E_{de} = \Delta E_{de,h} + \Delta E_{de,m} \quad (8.5)$$

$$\Delta E_{de,h} = \int T_0 h \cdot \frac{(\Delta T)^2}{T_a \cdot T_s} dA \quad (8.6)$$

$$\Delta E_{de,m} = \int T_0 h_v h_m \cdot \frac{\Delta T_{dew} \Delta \omega}{T_{a,dew} \cdot T_{s,dew}} dA \quad (8.7)$$

where A is the heat or mass transfer area; T_a and T_s are the temperatures of air and solution (in Kelvin); $T_{a,dew}$ and $T_{s,dew}$ are the absolute dew point temperatures of the air and solution, respectively; subscripts *h* and *m* of ΔE_{de} represent the exergy destructions of the heat transfer and mass transfer, respectively; ΔT and $\Delta \omega$ are temperature difference and humidity ratio difference between air and solution, respectively; h and h_m represent the convective heat transfer coefficient and mass transfer coefficient, respectively; and h_v denotes the latent heat of vaporization.

The exergy destruction of sensible heat transfer $\Delta E_{de,h}$ and that of moisture transfer $\Delta E_{de,m}$ could be expressed by ζ_h and ζ_m further, shown as Eqs. (8.8)–(8.9), respectively [16].

$$\Delta E_{de,h} \approx \frac{T_0}{T_a T_d} \cdot \frac{Q^2}{hA} \zeta_h, \text{ where } \zeta_h = \frac{\overline{\Delta T^2}}{\overline{\Delta T}^2} = \frac{\frac{1}{A} \int_A (\Delta T)^2 dA}{\left(\frac{1}{A} \int_A \Delta T dA\right)^2} \quad (8.8)$$

$$\Delta E_{de,m} \approx \frac{T_0 \lambda h_v}{T_{a,dew} T_{s,dew}} \cdot \frac{m_w^2}{h_m A} \zeta_m, \text{ where } \zeta_m = \frac{\overline{\Delta \omega^2}}{\overline{\Delta \omega}^2} = \frac{\frac{1}{A} \int_A (\Delta \omega)^2 dA}{\left(\frac{1}{A} \int_A \Delta \omega dA\right)^2} \quad (8.9)$$

where Q and m_w represent the sensible heat exchange and the moisture exchange, respectively; $\overline{\Delta T}$ and $\overline{(\Delta T)^2}$ are the average of ΔT and the average of ΔT^2 , respectively; $\overline{\Delta \omega}$ and $\overline{(\Delta \omega)^2}$ are the average of $\Delta \omega$ and the average of $\Delta \omega^2$, respectively; Q and m are the heat exchange amount and water transfer amount, respectively; and λ is the slope of the saturation line in a psychrometric chart, which is simplified to a constant. ζ_h or ζ_m is an index describing the distribution uniformity of ΔT or $\Delta \omega$, which is always greater than or equal to 1 [13]. Only when the ΔT or $\Delta \omega$ is constant, i.e., the driving force for heat or mass transfer is uniform, will ζ_h or ζ_m be equal to 1. The greater the value of ζ_h or ζ_m , the less uniform the heat or mass transfer driving force and the higher exergy destruction with a certain input hA .

Here, we choose a typical condition for these two basic types to investigate system performance. The parameters of the inlet outdoor air are 32 °C, 18 g/kg, and 1.33 kg/s, and the required humidity ratio of the supplied air is 9.5 g/kg. The circulating solute of LiBr in the dehumidifier/regenerator is 1.5 kg/s, while the solute flowing between the dehumidifier and the regenerator is 0.2 kg/s. The input heat transfer capacities of the key components are identical for Basic Types I and II. For example, the UA of the air-cooled condenser in Basic Type I is equal to the UA of the solution-cooled condenser in Basic Type II. NTU_a of the air-cooled condenser in Basic Type I is 4.8, while NTU_s of the solution-cooled condenser in Basic Type II is 0.8. Input NTUs of regenerator, dehumidifier, evaporator and solution heat exchanger are 2.5, 2.5, 0.8 and 3, respectively.

The typical air handling processes shown are illustrated in Fig. 8.5 in a psychrometric chart, and the typical operating parameters of key components are shown in Fig. 8.6. As indicated by Figs. 8.5a, b, the coupled heat and mass transfer process in the regenerator of Basic Type I proceeds close to the isenthalpic line, while the process of Basic Type II is near the iso-concentration line of the liquid desiccant. As indicated by the simulation results shown in Figs. 8.5 and 8.6, there are significant discrepancies in the operating performances of Basic Types I and II due to the difference between heating the regeneration air and heating the solution.

The unmatched coefficients of key components for Basic Type I and Basic Type II in a typical condition are listed in Table 8.1. As indicated by the match properties of these components, the unmatched coefficients of the evaporator, the dehumidifier, and the heat exchanger are similar for Basic Types I and II. The unmatched coefficient of the dehumidifiers is 1.07 for these two HPLD systems, indicating that the unmatched flow rates and parameters have a relatively limited effect on the dehumidification process. For the condenser and regenerator, there is

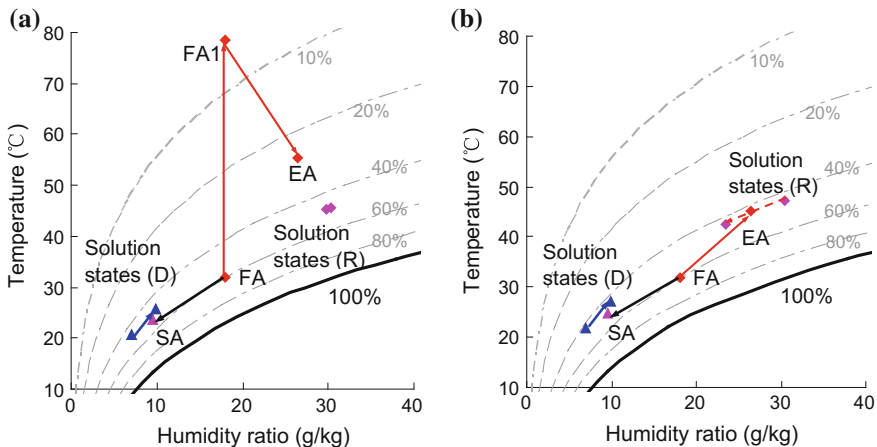


Fig. 8.5 Air and solution states of the heat pump-driven liquid desiccant air handling processes shown in a psychrometric chart: **a** Basic Type I; and **b** Basic Type II

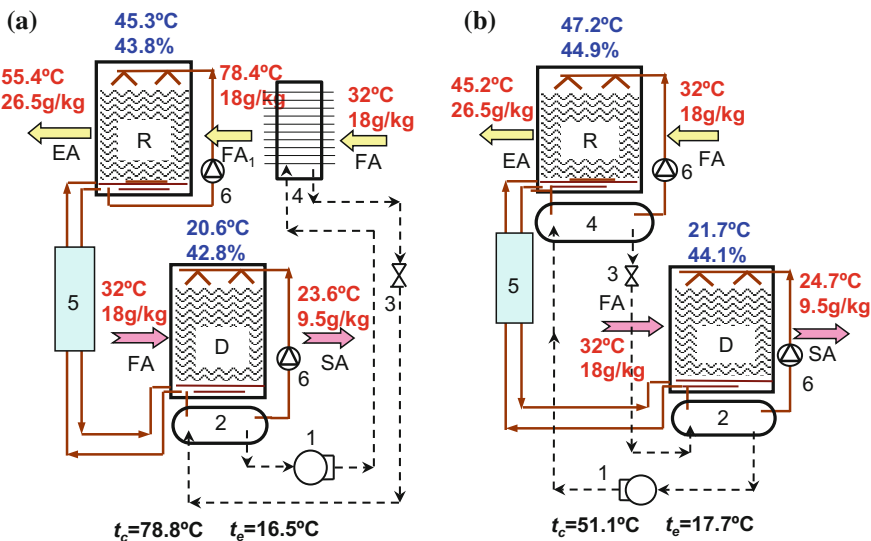


Fig. 8.6 Operating parameters of the HPLD systems in a typical condition: **a** Basic Type I; and **b** Basic Type II

significant variation in the unmatched coefficients of Basic Types I and II. In Basic Type I, ξ of the air-cooled condenser is 2.70 in this typical condition, more than two times higher than that of Basic Type II. This means that, for the air-cooled condenser of Basic Type I, the heat transfer resistance caused by the unmatched flow rates increases 170% on the basis of $1/UA$. As indicated by Fig. 8.5a, the regeneration air in Basic Type I has to be heated to a relatively high temperature to satisfy

Table 8.1 System performances of HPLD systems in a typical condition (fresh air: 32 °C, 18 g/kg)

Type	Unmatched coefficients ζ				Supply air	Performance of the heat pump cycle			
	Cond	Reg	Evap	Deh		t_c	t_e	COP_{hp}	COP_{sys}
Basic Type I	2.70	1.34	1.07	1.07	23.6 °C, 9.5 g/kg	78.8 °C	16.5 °C	1.89	1.83
Basic Type II	1.07	1.05	1.05	1.07	24.7 °C, 9.5 g/kg	51.1 °C	17.7 °C	4.53	4.17
Improved Type II	1.07 (1.07)	1.03 (1.07)	1.05 (1.05)	1.06 (1.08)	25.2 °C, 9.5 g/kg	49.6 °C (52.0 °C)	18.6 °C (18.7 °C)	4.70	4.32

Cond condenser; *Deh* dehumidifier; *Evap* evaporator; *Reg* regenerator

the requirement for desiccant regeneration before flowing through the regenerator, which leads to a high ζ of the air-to-solution condenser. As a result, the unmatched coefficient of the regenerator is 1.34, still significantly higher than that of Basic Type II. This implies that, in order to overcome the mass transfer resistance caused by unmatched flow rates and parameters, more heat and mass transfer capacity or a higher heat source temperature is required in Basic Type I compared to Basic Type II. In summary, the match properties of Basic Type II are much better than those of Basic Type I.

The significant difference in unmatched coefficients of Basic Types I and II is similar to the performance discrepancy between the simulated HPLD systems. The operating parameters of the HPLD systems in this typical condition are also listed in Table 8.1, including the evaporating and condensing temperatures of the heat pump, COP_{hp} , and COP_{sys} . The evaporating temperatures (t_e) and the supply air temperatures are similar for Basic Types I and II. However, the condensing temperature (t_c) of Basic Type I (78.8 °C) is much higher than that of Basic Type II (51.1 °C), indicating that the condensing temperature increases due to the unmatched flow rates of the air-cooled condenser. The increase of the condensing temperature results in a COP_{hp} of 1.89 in Basic Type I, lower than half of the COP_{hp} of Basic Type II (4.53).

As indicated by the analysis on match properties and simulated performances of HPLD systems, the handling process along the iso-concentration line is better than that along the isenthalpic line. And the process of heating the solution for regeneration is recommended over heating the regeneration air. The unmatched coefficients of key components in the HPLD systems help to evaluate the performance of the process, providing a relatively simple and effective method to guide the construction of an HPLD system. Thus, a principle for system construction is indicated based on the match property analysis: lower unmatched coefficients (ζ close to 1) mean the heat or mass transfer resistance caused by the unmatched flow rates or parameters is lower, and the system will demonstrate better energy performance. The unmatched coefficient based on exergy analysis can help to determine the key issues restricting the operating performance, providing the direction for constructing a better HPLD system. Compared with the system simulation method, the match property method is more simple and feasible.

To improve the performance of the HPLD system further, grading is proposed as an approach. Figure 8.7a gives the operating schematic of a two-stage HPLD system (Improved Type II), and the typical air handling process is shown in Fig. 8.7b. In contrast to Basic Type II, there are two-stage dehumidifier/regenerator and heat pump cycles in Improved Type II. The humid fresh air flows through

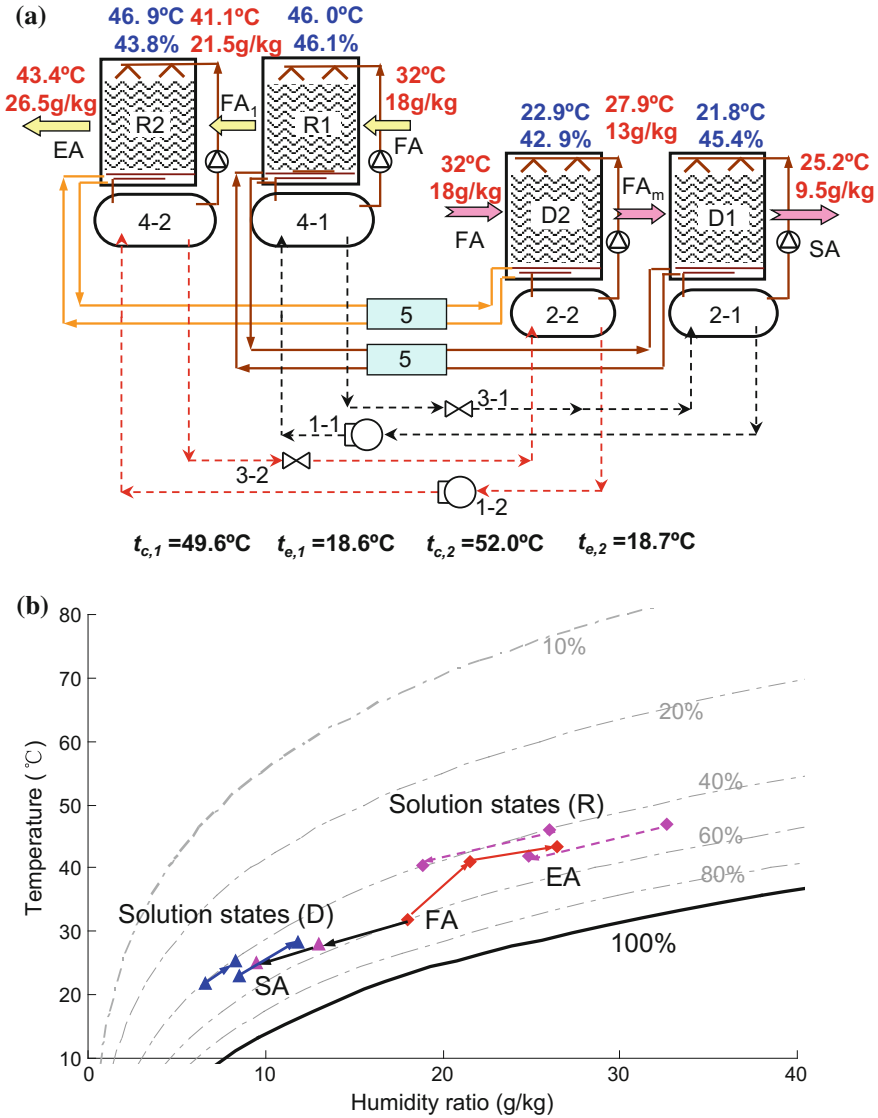


Fig. 8.7 Operating principle of Improved Type II: a system schematic; and b air handling process shown in a psychrometric chart

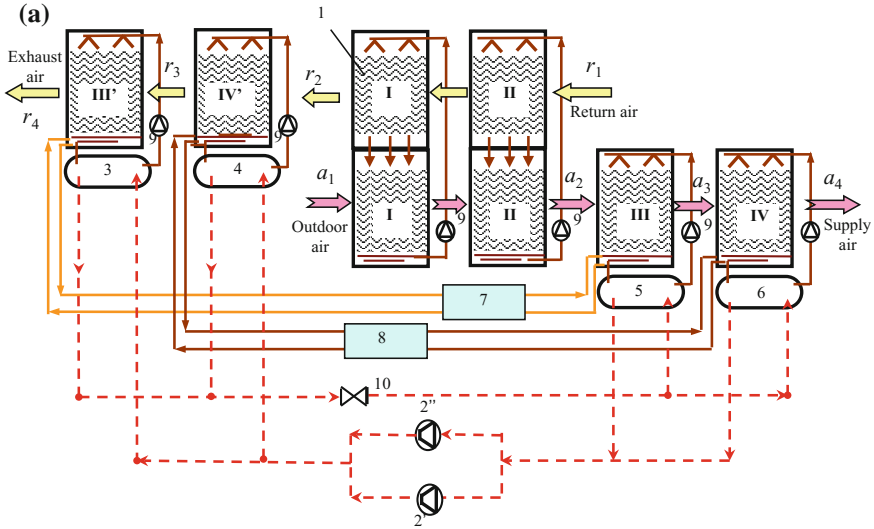
dehumidifiers D2 and D1 successively and is then dehumidified to the required state, while the regeneration air flows through regenerators R1 and R2 step-by-step for desiccant regeneration. The operating parameters of this two-stage HPLD system are also given in Fig. 8.7a, with the same fresh air parameters and required humidity ratio of the supply air analyzed previously. The unmatched coefficients of the key components and system operating performance of this improved system are listed in Table 8.1. The parameters in the brackets of Table 8.1 are the unmatched coefficients and performance parameters of the second stage.

As indicated by the match properties of this two-stage HPLD system, ξ_M of the regenerator or the dehumidifier for the first stage is a bit lower than in Basic Type II, but for the second stage, it is a bit higher. There is no significant difference between the unmatched coefficients of Basic Type II and Improved Type II. The simulated operating performances of this system confirm the results from the analysis of match properties. The condensing temperature of the first stage in Improved Type II is a bit lower than in Basic Type II, but that of the second stage is a bit higher. COP_{hp} of Improved Type II in this typical condition is 4.70, a bit higher than that of Basic Type II. Thus, compared with Basic Type II, the grading method (Improved Type II) leads to an improvement in the operating performance of the HPLD system. Thus utilizing the condensing heat to heat solution for regeneration is recommended rather than heating the regeneration air. And a multi-stage scenario is also recommended in the HPLD system to improve the system performance.

8.2.2 Tested Performance of Liquid Desiccant Outdoor Air Handling Processors

For liquid desiccant outdoor air handling processors operating in summer, the outdoor air is dehumidified in the dehumidifier and then the diluted solution is regenerated in the regenerator. According to whether there is indoor exhaust air that can be adopted as regeneration air, a distinction can be made between two different kinds of outdoor air handling processors that use liquid desiccant. If there is sufficient indoor exhaust air, the processor with enthalpy recovery from the indoor exhaust air and the process of utilizing the indoor exhaust air for desiccant regeneration could be adopted for outdoor air dehumidification. Alternatively, if there is not sufficient indoor exhaust air to be utilized directly, outdoor air could be adopted as the regeneration air, and a process using high-temperature chilled water to precool the outdoor air could be constructed to improve the performance of the outdoor air handling process. The following subsection examines the performance of the liquid desiccant outdoor air handling processors with indoor exhaust air as regeneration air. In such processors, the exhaust heat from the condenser is utilized to heat the desiccant coming into the regenerator, so the air handling processes are close to the iso-relative humidity line (rather than the isenthalpic line).

Figure 8.8 demonstrates the operating principle of a two-stage heat pump-driven liquid desiccant outdoor air processor operating in summer, which is composed of a two-stage enthalpy recovery device (spray modules numbered I and II), a two-stage dehumidifier/regenerator, and a vapor compression refrigeration cycle. In this figure, the straight lines and dashed lines stand for liquid desiccant and refrigerant, respectively. The top channel is for the indoor exhaust air, and the bottom channel is for the outdoor air. The outdoor air first enters the two-stage enthalpy recovery



1-heat recovery module; 2-compressor; 3-condenser I; 4-condenser II; 5-evaporator I; 6-evaporator II; 7-plate heat exchanger I; 8-plate heat exchanger II; 9-solution pump; 10-expansion valve

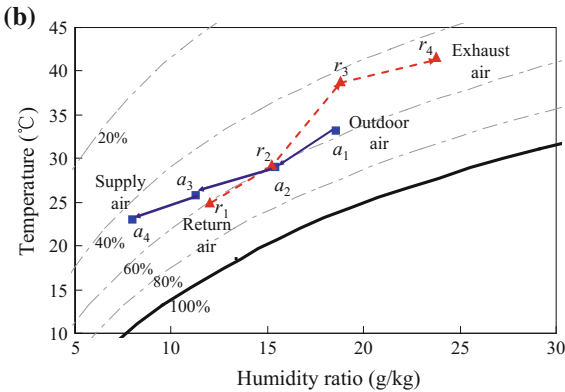


Fig. 8.8 Summer operation principle of the two-stage liquid desiccant outdoor air processor with enthalpy recovery: a operating schematic; and b air handling process

device and then flows into the evaporator-cooled two-stage dehumidification modules (numbered III and IV) before being supplied into occupied spaces. In the same way, the indoor exhaust air first enters the enthalpy recovery device and then flows into the condenser-heated modules (numbered IV' and III') before being exhausted to the outdoor environment. The evaporator of the heat pump is adopted to further cool and dehumidify the outdoor air coming out of the enthalpy recovery device to the desired supplied temperature and humidity ratio.

The liquid desiccant in this outdoor air processor is divided into two parts. One part is stored in spray modules I and II (in Fig. 8.8) for the purpose of enthalpy recovery, the equivalent state of which is decided by the outdoor air and the indoor exhaust air simultaneously. The other part is stored in spray modules III, III', IV and IV' to exchange heat with the evaporator and condenser, respectively. Taking the solution circulating between spray modules III and III' as an example to illustrate the operating principle in summer, the solution is first cooled by the evaporator (labeled 5 in Fig. 8.8a), and then exchanges heat and mass with the outdoor air in spray module III, where the solution is diluted and heated. The solution heated by the condenser (labeled 3 in Fig. 8.8a) enters spray module III' to be regenerated. The diluted solution and the regenerated solution are connected by solution pipes, and a plate heat exchanger (labeled 7 in Fig. 8.8a) is adopted for the internal heat recovery of the solution. The principle of spray modules IV and IV' is similar to that of modules III and III'. It is obvious that the enthalpy recovery device can efficiently reduce the energy consumption of the outdoor air handling processor. The cooling capacity and condensation heat of the heat pump are both effectively utilized in this outdoor air processor. Two parallel compressors are utilized in the heat pump cycle to operate efficiently under the partial load condition, so that the processor can have higher energy efficiency and control accuracy at partial load.

1. Tested performance at full load (typical hot and humid condition)

Because the heat pump system in the outdoor air processor utilizes two compressors working in parallel, and the solution in each stage exchanges heat with an individual evaporator (condenser), the dehumidification requirement at partial load can be achieved by adjusting the on-off time of these two compressors. As the required cooling temperature of the solution is about 15–20 °C, the evaporating temperature can be increased to about 7 °C. Meanwhile, the condensing temperature is only around 45 °C since the required heating temperature of the solution is about 40 °C. The test results of the outdoor air processor shown in Fig. 8.8 under the summer design condition are listed in Table 8.2. The coefficient of performance COP_{air} is defined as

$$COP_{air} = \frac{\text{Cooling capacity of the outdoor air}}{\text{Power consumption of compressor and solution pumps}} \quad (8.10)$$

The COP of the heat pump (COP_{hp}) in the outdoor air processor is 4.0, while COP of the processor (COP_{air}) is as high as 5.0.

Table 8.2 Test results of the outdoor air processor under the summer design condition

Parameter	Unit	Value	Parameter	Unit	Value
Outdoor air flow rate	m ³ /h	4058	Exhaust air flow rate	m ³ /h	4021
Outdoor air dry-bulb temperature	°C	36.0	Return air dry-bulb temperature	°C	26.0
Outdoor air humidity ratio	g/kg	25.8	Return air humidity ratio	g/kg	12.6
Supply air dry-bulb temperature	°C	17.3	Exhaust air dry-bulb temperature	°C	39.1
Supply air humidity ratio	g/kg	9.1	Exhaust air humidity ratio	g/kg	38.6
Evaporating temperature	°C	7.0	Condensing temperature	°C	45.0
Power consumption of the compressors	kW	14.6	Power consumption of the solution pump	kW	1.92
Outdoor air cooling capacity	kW	82.7	Exhaust air heating capacity	kW	101.9
Outdoor air dehumidification rate	kg/h	80.1	Cooling capacity of the heat pump	kW	59.0
COP _{air}	W/W	5.0	COP _{hp} of the heat pump	W/W	4.0

2. Tested performance and analysis at partial load (summer)

Based on the test results under the design condition, performance of the processor at partial load was then tested, and the main results are listed in Table 8.3. Since only one compressor is in operation at partial load, while the heat transfer area of the evaporator and that of the condenser are identical, the heat transfer between the refrigerant and the solution became more sufficient and the heat transfer temperature differences decrease accordingly. As a result, the evaporating temperature rises and the condensing temperature drops. As indicated by the test results listed in Table 8.3, the evaporating temperature increases to 11 °C, while the

Table 8.3 Test results of the outdoor air processor at partial load under the summer condition

Parameter	Unit	Value	Parameter	Unit	Value
Outdoor air flow rate	m ³ /h	4058	Exhaust air flow rate	m ³ /h	4021
Outdoor air dry-bulb temperature	°C	30.0	Return air dry-bulb temperature	°C	26.0
Outdoor air humidity ratio	g/kg	17.4	Return air humidity ratio	g/kg	12.7
Supply air dry-bulb temperature	°C	17.3	Exhaust air dry-bulb temperature	°C	39.1
Supply air humidity ratio	g/kg	9.6	Exhaust air humidity ratio	g/kg	26.6
Evaporating temperature	°C	11.0	Condensing temperature	°C	37.6
Power consumption of the compressors	kW	5.8	Power consumption of the solution pump	kW	1.43
Outdoor air cooling capacity	kW	42.7	Cooling capacity of the heat pump	kW	33.2
COP _{air}	W/W	5.9	COP _{hp} of the heat pump	W/W	5.7

condensing temperature decreases by 7.4 °C compared to the full-load condition to 37.6 °C. Thus, COP_{hp} and COP_{air} increase to 5.7 and 5.9, respectively. As the outdoor air handling processor was running at partial load for more than 70% of the time, the comprehensive energy efficiency of this liquid desiccant processor could be as high as 5.5.

Based on these test results, it can be seen that the heat pump-driven liquid desiccant outdoor air processor can effectively meet the dehumidification requirement in summer with high comprehensive energy efficiency. The humidity ratio of the dehumidified outdoor air can meet the demand for humidity control with the supply air temperature around 17 °C, which could be supplied directly into the conditioned room without further reheating or cooling. Moreover, the enthalpy recovery modules are adopted in this process to recover energy from the indoor exhaust air. In summary, the outdoor air processor can meet the needs of running at full load and partial load with comprehensive energy efficiency up to 5.5.

8.2.3 Applications of Liquid Desiccant System in Buildings

Temperature and humidity independent control (THIC) air-conditioning system is proposed as an efficient air-conditioning system [8]. Figure 8.9 illustrates the operating principle of the THIC air-conditioning system, with an outdoor air handling subsystem and a relatively high-temperature cooling source subsystem that can separately regulate the indoor temperature and humidity, respectively. As indoor temperature and humidity are regulated by independent subsystems, the THIC system can satisfy the variance of the indoor heat moisture ratio. Therefore, the THIC system can avoid the imbalance of indoor parameters, and it addresses the conventional system’s inability to meet temperature and humidity requirements simultaneously.

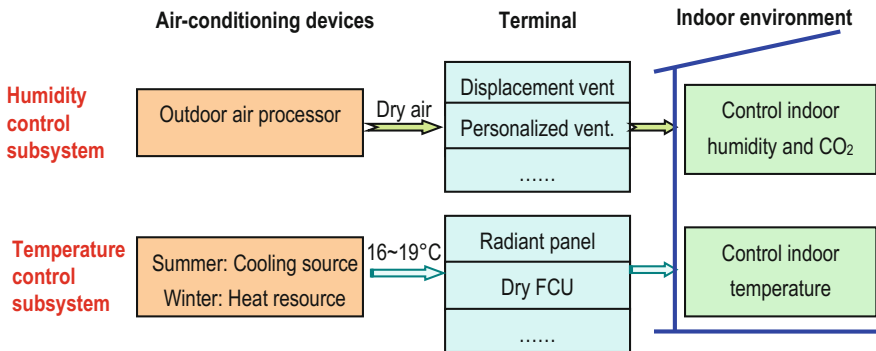


Fig. 8.9 Operating principle of the THIC air-conditioning system

HPLD systems could be applied as the humidity control device in the THIC system. It is responsible for dehumidifying humid air and supplying dry air to the indoor space. There have been numerous applications using HPLD systems in China. An office building will be taken as an example in this section.

8.2.3.1 Basic Information

A 5-story office building, as shown in Fig. 8.10, is located in Shenzhen, China, with total building area of 21,960 m² and the areas of 5940, 5045, 3876, 3908, 3191 m² for the 1st to 5th floor, respectively. The main functions of the 1st floor are mess hall, archive and carport, while the 2nd to 4th floors are the office rooms, with the 5th floor as the meeting room. And there is a vestibule vertically through up the 2nd to 4th floors in the north of this building.

The outdoor condition in Shenzhen is rather hot and humid all through the year. The annual outdoor air relative humidity is about 80% and humidity ratio in summer is as high as 20 g/(kg dry air). The building requires both cooling and dehumidification in a long period of time, and no heating and humidification requirement in winter. Therefore, how to handle the moisture efficiently is the key issue in such a subtropical area.

The THIC system serves from 1st to 4th floor with the net air-conditioning area of 13,180 m² (the total area of 18,769 m²), and the 5th floor is served by several stand-alone air-conditioners and is not within the scope of our discussion. The schematic of the THIC system is represented in Fig. 8.11 with the parameters of main devices in the humidity control subsystem listed in Table 8.4.

The right side of Fig. 8.11 is the humidity control subsystem, including 9 liquid desiccant outdoor air handling units that supply adequate dry outdoor air into the occupied spaces. As the flow rate of the supplied outdoor air is proportional to the



Fig. 8.10 The tested office building in Shenzhen

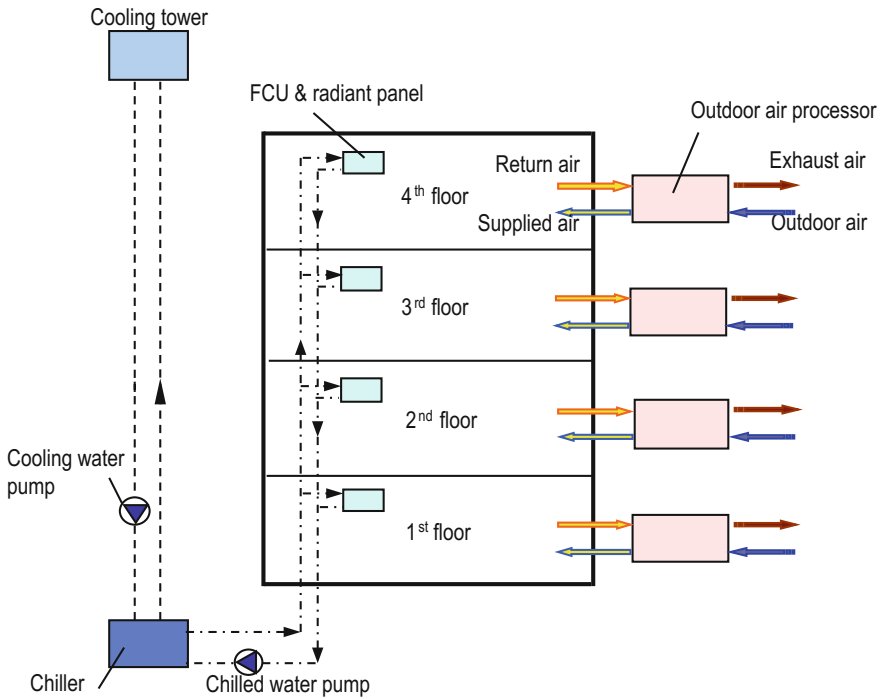


Fig. 8.11 Schematic of the THIC air-conditioning system

Table 8.4 Main devices of the humidity control system in the office building

Subsystem	Device	Rated parameters
Humidity control subsystem	Outdoor air handling units	Fresh air flow rate 2000 m ³ /h, cooling capacity 39 kW, power consumption ^a 10 kW; for offices in the 4th floor
		Fresh air flow rate 4000 m ³ /h, cooling capacity 83 kW, power consumption ^a 25 kW; for offices in the 4th floor
		Fresh air flow rate 5000 m ³ /h, cooling capacity 103 kW, power consumption ^a 28 kW; 2 units for the 2nd floor, and 2 units for the 3rd floor
		Fresh air flow rate 8000 m ³ /h, cooling capacity 166 kW, power consumption ^a 45 kW, for vestibule in the 2nd floor
		Fresh air flow rate 10000 m ³ /h, cooling capacity 196 kW, power consumption ^a 45 kW, for restaurant in the 1st floor

^aIncluding power consumption of compressors, solution pumps, and fans inside the outdoor air units

number of people, the pollutants, CO₂ and latent heat produced by human bodies can be removed by outdoor air. The schematic of the heat pump-driven outdoor air processors using liquid desiccant is illustrated in Fig. 8.8, which is composed of a two-stage enthalpy recovery device and a two-stage air handling device coupled with refrigeration cycles. LiBr aqueous solution is employed as liquid desiccant in these air processors. The enthalpy recovery device is used to recover the energy from indoor exhaust air to decrease the energy consumption of the outdoor air handling process. And in the heat pump-driven air handling device, the diluted solution from the dehumidification modules is heated by the exhaust heat from the condenser and concentrated in the regeneration modules. Then, the hot concentrated solution is cooled by passing through the heat exchanger and evaporator before it enters the dehumidification modules, and lastly used to remove moisture from the outdoor air.

8.2.3.2 Energy Efficiency of Humidity Control Subsystem

The performances of the liquid desiccant outdoor air units were tested one by one on May 27, 2009, according to the measured flow rates, air inlet and outlet parameters through the processor and input power of compressors, solution pumps and fans. The tested results of seven outdoor air units are summarized in Table 8.5; the other two processors are neglected due to the difficulty of installing the sensors.

The east side processor of the 2nd floor is a typical example for the outdoor air unit, and its specific operation information is shown in Table 8.6. The outdoor air flow rate was 5059 m³/h, the outdoor air parameters were 29.3 °C and 20.3 g/kg, and the supply air parameters were 17.1 °C and 6.2 g/kg. So the cooling capacity (Q_{air}), calculated by energy balance equation, was 82.6 kW. The power consumption of compressors together with solution pumps (P_{air}) inside the processor was 17.8 kW, and the power consumption of the supply air and exhaust air fans (P_{fan}) was 2.2 kW. Therefore, the performance of the outdoor air unit (COP_{air}), the transport coefficient of fans (TC_{fan}) and the performance of the entire humidity handling process (COP_{hum}), as shown in Eqs. (8.11)–(8.13), are 4.7, 37.5 and 4.2, respectively.

$$\text{COP}_{\text{air}} = \frac{Q_{\text{air}}}{P_{\text{air}}} \quad (8.11)$$

$$\text{TC}_{\text{fan}} = \frac{Q_{\text{air}}}{P_{\text{fan}}} \quad (8.12)$$

$$\text{COP}_{\text{hum}} = \frac{Q_{\text{air}}}{P_{\text{air}} + P_{\text{fan}}} \quad (8.13)$$

Table 8.5 Performance of the outdoor air handling units (outdoor condition: 29.3 °C and 20.3 g/kg)

Location	Supply outdoor air		Cooling capacity/kW		Power consumption/kW		COP _{air}	TC _{fan}	COP _{hum}
	Flow rate/ (m ³ /h)	Temperature/ C	Humidity ratio/(g/kg)	Compressors and solution pumps	Fans				
East side of 2nd floor	5059	17.1	6.2	82.6	17.8	2.2	4.7	37.5	4.2
West side of 2nd floor	5195	16.7	6.1	86.0	17.6	2.3	4.9	37.4	4.3
East side of 3rd floor	4972	16.8	6.5	80.4	18.2	2.2	4.4	36.5	4.0
West side of 3rd floor	5215	16.6	6.2	86.4	17.6	2.2	4.9	39.3	4.4
East side of 4th floor	4261	16.7	6.4	69.5	15.0	1.7	4.6	40.9	4.2
Middle side of 4th floor	1940	16.5	6.2	32.1	7.1	0.9	4.5	35.7	4.0
West side of 4th floor	4307	16.3	6.1	72.0	15.3	1.8	4.7	40.0	4.2

Table 8.6 Operation condition of a typical outdoor air handling unit (east side of 2nd floor)

Outdoor condition	Supplied outdoor air	Stage	Evaporating temperature/°C	Condensing temperature/°C	Solution parameter (temperature and concentration)
Temperature: 29.3 °C Humidity ratio: 20.3 g/kg	Temperature: 17.1 °C Humidity ratio: 6.2 g/kg Flow rate: 5059 m ³ /h	I	11.0	50.8	Dehumidification module
					Inlet: 15.8 °C, 34.6%
					Outlet: 20.5 °C, 34.4%
		II	4.4	51.3	Regeneration module
					Inlet: 44.2 °C, 34.9%
					Outlet: 38.3 °C, 35.2%
II	4.4	51.3	Dehumidification module		
			Inlet: 9.0 °C, 44.1%		
			Outlet: 14.0 °C, 43.9%		
II	4.4	51.3	Regeneration module		
			Inlet: 44.3 °C, 44.8%		
			Outlet: 37.9 °C, 45.1%		

As shown in Table 8.5, the COP_{air} of the tested seven outdoor air units were in the range of 4.4–4.9, the TC_{fan} of the fans were 35–40, and the COP_{hum} of the entire humidity handling processes were 4.0–4.4.

According to the tested data and rated parameters of the outdoor air units and fans, the calculated cooling capacity of the entire humidity control subsystem was 773.0 kW with total inside compressors and solution pumps input power of 166.9 kW and total fans input power of 20.0 kW, so the coefficient of performance of the humidity control subsystem (COP_{HUM}), shown in Eq. (8.14), is 4.1.

$$COP_{HUM} = \frac{\sum Q_{air}}{\sum (P_{air} + P_{fan})} \quad (8.14)$$

Similarly, on the basis of the tested data of another day, the COP_{HUM} under the design condition was 4.1, with the calculated cooling capacity of 915.0 kW, total inside compressors and solution pumps input power of 194.4 kW and total fans input power of 25.1 kW.

8.2.3.3 Energy Performance of the Entire THIC System

Calculated from the above tested data, the overall COP of the THIC system (COP_{SYS}) under partial load condition and design condition were 4.0 and 4.1, respectively, as shown in Eq. (8.15).

$$COP_{SYS} = \frac{Q_{CH} + \sum Q_{air}}{(P_{CH} + P_{CT} + P_{CTP} + P_{CWP} + P_{FCU}) + \sum (P_{air} + P_{fan})} \quad (8.15)$$

where Q_{CH} refers to the cooling capacity of water chiller; $\sum Q_{air}$ indicates the sum of cooling capacities of outdoor air handling processors using liquid desiccant; P_{CH} , P_{CT} , P_{CTP} , P_{CWP} and P_{FCU} represent the power consumptions of water chiller, cooling tower, cooling water pump, chilled water pump and FCU, respectively. P_{air} and P_{fan} represent the power consumptions of outdoor air handling processors and fans for air supply, respectively.

Based on the tested results of these two typical operating conditions, it is convinced that the THIC system in this office building has achieved a high efficiency with its total COP over 4.0. By comparison, the measured average coefficient of performance of whole system in traditional fan-coil systems is usually around 3.0. Therefore, there is a remarkable energy efficiency improvement of the THIC system comparing with the conventional system.

Energy consumption of the THIC system was measured by the power metering monitoring system. Figure 8.12 shows the monthly power consumption of the system from 15 April to 15 October (apart from weekends and statutory holidays). The total energy consumption was 425,000 kWh during the cooling season, and the humidity control subsystem occupied 61% of the total power consumption which

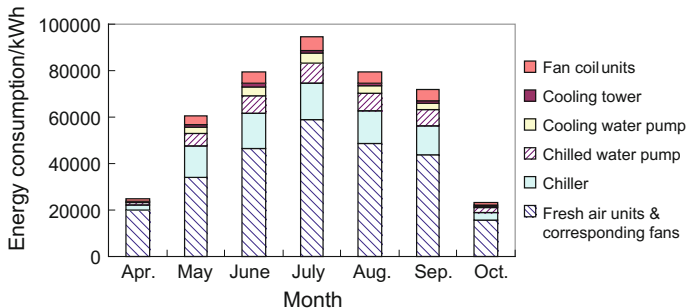


Fig. 8.12 Monthly power consumption of the THIC system

was proportional to the ratio of cooling load that the humidity control subsystem undertook.

The annual energy consumption in unit building area and unit net air-conditioning area of the tested THIC system were 22.6 kWh/(m² year) and 32.2 kWh/(m² year), respectively. However, the average energy consumption levels of office building of the similar building envelope and occupant density during the same time in Shenzhen were around 42–49 kWh/(m² year) according to the investigated results. Therefore, the THIC system in this office building achieved noticeable energy saving in operation compared with the conventional air-conditioning system, and the added cost can be recalled within two years.

8.3 Air Handling Process Using Desiccant Wheel

The DW, the subsidiary cooling systems and the heating devices are three main parts of a typical DW-based air handling system. Heating devices can be electrical heating, gas burner, solar energy, heat pump systems, etc., depending on regeneration temperature T_r . T_r is influenced not only by the DW, but also by the cooling method. As for the DW, its performances are influenced by a variety of parameters, such as the wheel’s dimensions and the structure of air channels, rotation speed, inlet states of the air, regeneration air mass flow rate, area ratio of regeneration section, purge section, etc. Tu et al. [17] found that, when the wheel’s structure and working conditions are fixed, the lowest T_r can be achieved for DWs with the facial area ratio and the air flow rate ratio of the two streams of air being both equal to 1. In this section, performances of a one-stage system and a two-stage system with identical heat transfer areas are compared, with particular emphasis on the required heating source temperature. Heat pump cycle is utilized for desiccant regeneration, and the condensing temperature is regarded as the heating source temperature.

8.3.1 Operating Principle of the Heat Pump-Driven Multi-stage DW System

The operating principle of the heat pump-driven multi-stage DW system is depicted in Fig. 8.13 (taking 2-stage as an example). For the N -stage system, there are N DWs and one heat pump system, with $N + 1$ condensers being used as heaters and N evaporators being used as coolers. Taken the two-stage system in Fig. 8.13 as an example, the operating principle are as follows. The processed air is dehumidified by DW 1 ($A_{Pin}-A_{P1}$) before flowing into evaporator 1 to be cooled ($A_{P1}-A_{P2}$). After being dehumidified by DW 2 ($A_{P2}-A_{P3}$), it is cooled by evaporator 2 ($A_{P3}-A_{Pout}$) before being introduced into occupied spaces. The regeneration air is heated by condenser 2 ($A_{Rin}-A_{R1}$), humidified by DW 2 ($A_{R1}-A_{R2}$), heated by condenser 1 ($A_{R2}-A_{R3}$), humidified by DW 1 ($A_{R3}-A_{R4}$), and finally used to dissipate the extra heat from condenser 0 ($A_{R4}-A_{Rout}$) before being exhausted to the outdoor environment. The air handling processes of the heat pump-driven one-stage and two-stage desiccant dehumidification system are shown in psychrometric chart in Fig. 8.14. Compared with one-stage system, during this stage-by-stage dehumidification process of the multi-stage system, the processed air is cooled down before the temperature rises too high in the wheel. Thus, the processed air can remain in a low temperature range, which ensures that the desiccant can stay in a low temperature range. Furthermore, the desiccant water content can be relatively higher while still reaching the same supplied air humidity ratio, and the corresponding regeneration temperature can be reduced as well.

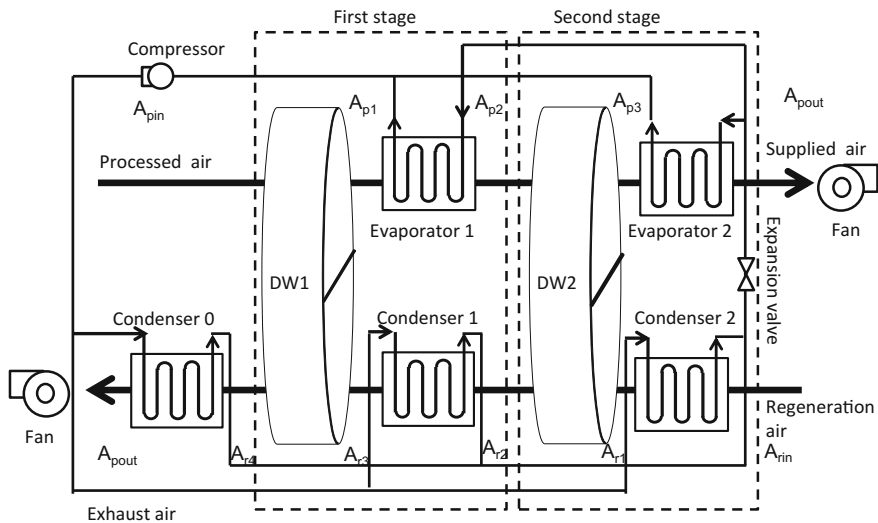


Fig. 8.13 Schematic of a heat pump-driven two-stage DW cooling system

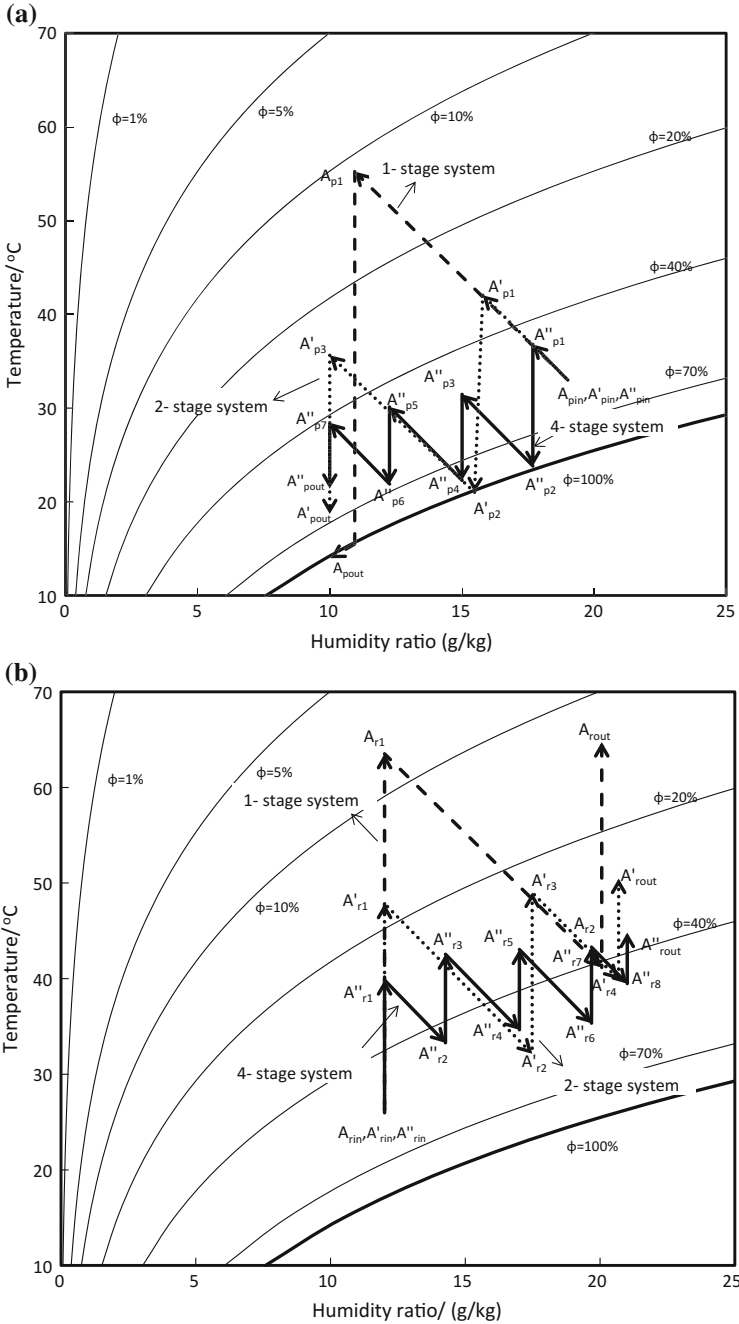


Fig. 8.14 Air handling process with different numbers of stages: **a** processed air; and **b** regeneration air

For heat pump-driven systems, power input from the compressor is required to transfer heat from evaporators to condensers. The coefficient of performance of this system (COP_R) is calculated by dividing the cooling capacity of the processed air (Q_c) by the power input of the compressor (E_c), as shown as:

$$COP_R = \frac{m_p(i_{pin} - i_{pout})}{P} = \frac{m_p(i_{pin} - i_{pout})}{Q_c} \frac{T_{evap}}{T_{cond} - T_{evap}} \varepsilon \quad (8.16)$$

Q_c is calculated by the enthalpy variance of the processed air and the mass flow rate of the processed air (m_p).

8.3.2 Performances of the Heat Pump-Driven Multi-stage DW System

In this section, the influences of the number of stages on COP_R of the heat pump-driven DW system are investigated, with the same entire heat and mass transfer areas for different systems. The thickness of the DW and the heat transfer area of all the heat exchangers, i.e., evaporators and condensers are evenly divided in the multi-stage system. The wheel's facial area is evenly divided for dehumidification and regeneration. The operating conditions and component information are shown in Table 8.7. For all systems and cases, the DWs are operated at the optimum rotation speeds. In this way, the required heat source temperatures can be evaluated and compared.

The influences of stage number on the performances of the system are shown in Fig. 8.15. It can be seen that, when the supplied humidity ratio is fixed at 10 g/kg, as the increase of stage number, the change of supplied air temperature is not obvious. However, the evaporating temperature is increasing and the condensing temperature, which is also the heat source temperature, is decreasing. This is beneficial for the increase of COP_R , since the work of the compressor (P) is reducing when the total heat change of the processed air (Q_c) is almost constant, according to Eq. (8.16). For one-stage, two-stage and four-stage systems, COP_R are 2.41, 3.74 and 4.50, respectively.

In the next part, the reasons behind the fact that heat pump-driven multi-stage DW system has higher performances than single-stage system will be explained

Table 8.7 Information related to working conditions, desiccant wheels, and the heat pump system

Operating conditions	DW	Heat pump system
Processed air: 33 °C, 19 g/kg, 0.8 kg/s	Radius: 0.5 m	Total air side NTU for evaporators (NTU _e): 5
Regeneration air: 26 °C, 12 g/kg, 0.8 kg/s	Total thickness: 0.2 m	Total air side NTU for condensers (NTU _h): 5
Supplied air: 10 g/kg	Material: silica gel	Thermodynamic perfectness of the compressor: 0.5
	Nu of air channels: 2.463	

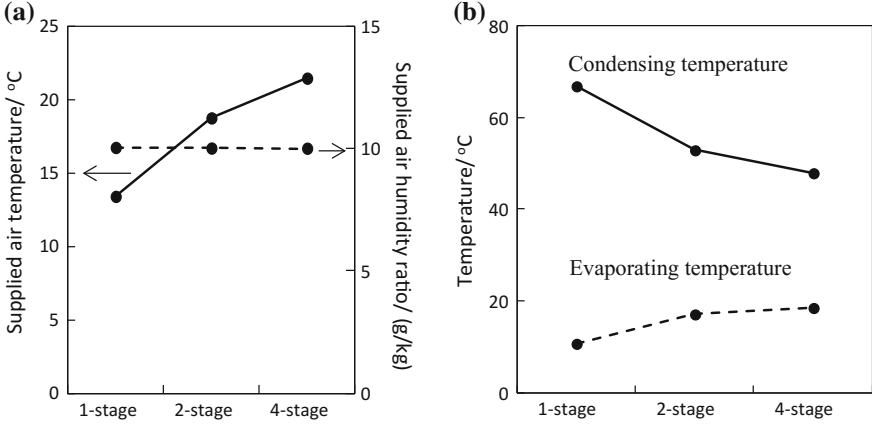


Fig. 8.15 Effect of the number of stages on: **a** supplied air temperature and humidity ratio; **b** evaporating temperature and condensing temperature

from the perspective of unmatched coefficients. And expressions of unmatched coefficients in heat and mass transfer processes between air and solid desiccant are the same as those between air and liquid desiccant expressed in Eqs. (8.8) and (8.9).

8.3.3 Theoretical Analysis Using Unmatched Coefficients

When the air is handled in the desiccant wheels and heat exchangers (i.e., evaporators and condensers), there exists heat and mass transfer exergy destruction because of the temperature and humidity ratio differences. Input power consumption P can be written as Eq. (8.17) [17].

$$P = m_p(e_{pout} - e_{pin}) + m_r(e_{rout} - e_{rin}) + \Delta E_{DW} + \Delta E_{HE} + \Delta E_e \quad (8.17)$$

where ΔE_{DW} and ΔE_{HE} are the exergy destruction of all the desiccant wheels and all the heat exchangers, respectively; and ΔE_e is the exergy destruction of the compressor, which is equal to $T_0(Q_{cond}/T_{cond} - Q_{evap}/T_{evap})$, resulting from thermodynamic perfectness (ε) of the compressor being lower than 1.

For the heat pump-driven multi-stage DW system, according to Eq. (8.17), under the fixed inlet and outlet states of the processed air, when exergy destruction decreases, P can also decrease. And it can be obtained from Eq. (8.16) that the condensing temperature (T_{cond}) is reduced and the evaporating temperature (T_{evap}) increases accordingly. In summary, the heat source temperature (T_{cond}) is determined by the required P . In order to reduce T_{cond} , the systems' exergy destruction should be reduced.

It is indicated the factors that influence the heat and mass transfer exergy destruction are heat and mass transfer capacities, heat and mass transfer area and unmatched coefficient. For the cases talked about in this part, the total heat and mass transfer area for each kind of component are identical and the total heat and mass transfer capacities are almost the same. Therefore, unmatched coefficients are the main performance influencing factor under different number of stages.

Figure 8.16 shows the exergy destructions under different number of stages. Table 8.8 listed the detailed information about unmatched coefficients and heat transfer capacities. As for the desiccant wheels, the unmatched coefficients for all

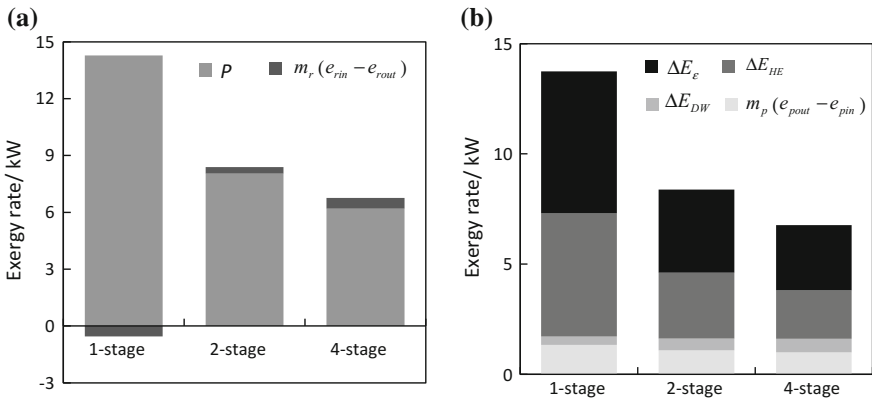


Fig. 8.16 Effect of the number of stages on: **a** exergy provided by the compressor and the regeneration air; **b** exergy destruction and exergy obtained by the processed air

Table 8.8 Heat and mass transfer capacities and unmatched coefficients in multi-stage desiccant wheel systems

	1-stage system	2-stage system	4-stage system
Unmatched coefficient of desiccant wheel	1.12 (Average)	1.10 (Average)	1.15 (Average)
Q_c /kW	36.1	18.8 (Evap. 1), 13.8 (Evap. 2)	10.8 (Evap. 1), 7.6 (Evap. 2), 6.7 (Evap. 3), 5.7 (Evap. 4)
Unmatched coefficient of evaporators	2.53 (Average)	1.47 (Average)	1.13 (Average)
Q_h /kW	19.6 (Cond. 0), 30.8 (Cond. 1)	8.8 (Cond. 0), 14.0 (Cond. 1), 17.9 (Cond. 2)	4.5 (Cond. 0), 6.6 (Cond. 1), 6.9 (Cond. 2), 7.6 (Cond. 3), 11.4 (Cond. 4)
Unmatched coefficient of condensers	1.47 (Average)	1.22 (Average)	1.08 (Average)
COP_R	2.41	3.74	4.50

the DWs in one system are almost the same. Therefore, only the average values are provided.

It can be seen from Fig. 8.16 that, as the number of stages increases, P decreases. The reduction of P mainly results from the reduction of both the exergy destruction of the evaporators and condensers (ΔE_{HE}) and the exergy destruction of the compressor (ΔE_c). The exergy destructions of desiccant wheels are almost constant. It can be seen from Table 8.8 that, as the number of stages increases from 1 to 4, the unmatched coefficients of the DW vary little. However, those for evaporators and condensers decrease from 2.53 to 1.13 and from 1.47 to 1.08. The exergy destruction of all the evaporators (or condensers) decreases from 2.80 kW (or 3.06 kW) in the single-stage system to 1.36 kW (or 1.62 kW) in the two-stage system, and then to 0.97 kW (or 1.23 kW) in the four-stage system.

In conclusion, for the heat pump-driven multi-stage DW systems, as the number of stages increases, the condensing temperature, which represents the heat source temperature, decreases; the unmatched coefficient and the exergy destruction decrease, too. Higher COP_R values can be obtained. When the number of stages is larger than 4, the rate of improvement slows down due to the insignificant change of the unmatched coefficient. A 4-stage system with COP_R around 4.5 is preferable.

8.4 Discussion

There are similarities for air dehumidification systems using LD and desiccant wheel (DW). The liquid desiccant and solid desiccant could both be presented in an air psychrometric chart. They are both coupled heat and mass transfer processes between air and desiccant. Temperature difference ΔT and humidity ratio difference $\Delta \omega$ between air and desiccant are the driving forces of heat and mass transfer processes, respectively. States of solution and solid desiccant are influenced with the adsorption or desorption of latent heat of vaporization. A dehumidification and regeneration process is of the essence to complete the handling cycle using LD or DW. Heating source is also required to provide a sufficient driving force to realize the regeneration.

However, there are obvious distinctions between the air handling processes using LD and DW from the perspective of driving forces and system scenarios, which could be summarized as following.

1. Characteristics of the driving forces are different for the processes using LD and DW. ζ_h and ζ_m are approaching to 1, i.e., both ΔT and $\Delta \omega$ are relatively uniform in the DW process when the facial area ratio and the air flow rate of the two streams of air being both equal to 1. As for the LD process, the distribution of ΔT or $\Delta \omega$ is influenced by the inlet states of air and solution; ζ_h and ζ_m could be approaching to 1 only when the inlet air is near the desiccant iso-concentration line.

2. The regeneration process in LD system is similar to that in the DW system if heating source is adopted to heat the regeneration air. However, solution could be heated for regeneration in the LD process attributing to the liquidity of fluid. Unmatched coefficient is reduced to a great extent and a regeneration process approaching to the iso-concentration line is realized, which is beneficial to lower the regeneration temperature of liquid desiccant systems.
3. Air handling process in the DW system is always approaching to the isenthalpic line. Although the driving forces between air and solid desiccant are relatively uniform, the regeneration temperature of the DW process is fairly high due to the isenthalpic process. A multi-stage process using DW is helpful to lower the required heating source temperature.
4. Besides, there are also distinctions in configurations of the air handling processes using LD and DW. For example, a solution–solution heat exchanger could be set in the LD process, which is responsible to recover heat between the solutions circulating between the regenerator and the dehumidifier. Air–air heat exchanger is recommended between the processed air out of the DW and the inlet regeneration air, which could be used for preheating the regeneration air. However, in DW system, desiccant material directly enters the regeneration region or the dehumidification region after dehumidification or regeneration, which leads to unavoidable heat and cold offset due to the rotation of DW [11].

References

1. THUBERC (2015) Status quo of building energy consumption in China. In: 2015 annual report on China building energy efficiency. China Architecture & Building Press, Beijing, pp 1–39
2. Al-Alili A, Hwang Y, Radermacher R (2015) Performance of a desiccant wheel cycle utilizing new zeolite material: experimental investigation. *Energy* 81:137–145
3. Enteria N, Yoshino H, Mochida A et al (2015) Exergoeconomic performances of the desiccant-evaporative air-conditioning system at different regeneration and reference temperatures. *Int J Refrig* 56:81–98
4. Nawaz K, Schmidt SJ, Jacobi AM (2015) A parametric study on mass diffusion coefficient of desiccants for dehumidification applications: silica aerogels and silica aerogel coatings on metal foams. *Sci Technol Built Environ* 21:637–647
5. Bellemo L, Elmegaard B, Kærn MR et al (2015) Formulation and validation of a two-dimensional steady-state model of desiccant wheels. *Sci Technol Built Environ* 21:300–311
6. Chua KJ (2015) Heat and mass transfer of composite desiccants for energy efficient air dehumidification: modelling and experiment. *Appl Therm Eng* 89:703–716
7. De Antonellis S, Intini M, Joppolo CM (2015) Desiccant wheels effectiveness parameters: correlations based on experimental data. *Energ Build* 103:296–306
8. Liu XH, Jiang Y, Zhang T (2013) Key components of the THIC system: outdoor air handling methods. Temperature and humidity independent control (THIC) of air-conditioning system. Springer Press, Berlin, pp 119–153
9. Liu XH, Li Z, Jiang Y (2009) Similarity of coupled heat and mass transfer between air–water and air–liquid desiccant direct-contact systems. *Build Environ* 44:2501–2509

10. Liu XH, Jiang Y, Xia JJ et al (2007) Analytical solutions of coupled heat and mass transfer processes in liquid desiccant air dehumidifier/regenerator. *Energ Convers Manage* 48:2221–2232
11. Tu R, Liu XH, Jiang Y (2013) Performance comparison between enthalpy recovery wheels and dehumidification wheels. *Int J Refrig* 36:2308–2322
12. Zhang T, Liu XH, Jiang Y (2012) Performance optimization of heat pump driven liquid desiccant dehumidification systems. *Energ Build* 52:132–144
13. Zhang T, Liu XH, Jiang Y (2013) Performance comparison of liquid desiccant air handling processes from the perspective of matched properties. *Energ Convers Manage* 75:51–60
14. Bejan A (1997) *Advanced engineering thermodynamics*, 2nd edn. Wiley, New York
15. Zhang L, Liu XH, Jiang Y (2014) Exergy calculation and analysis of a dehumidification system using liquid desiccant. *Energ Build* 69:318–328
16. Liu XH, Zhang T, Zheng YW et al (2016) Performance investigation and exergy analysis of two-stage desiccant wheel systems. *Renew Energ* 86:877–888
17. Tu R, Liu XH, Jiang Y (2015) Lowering the regeneration temperature of a rotary wheel dehumidification system using exergy analysis. *Energ Convers Manage* 89:162–174